



저작자표시-비영리-변경금지 2.0 대한민국

이용자는 아래의 조건을 따르는 경우에 한하여 자유롭게

- 이 저작물을 복제, 배포, 전송, 전시, 공연 및 방송할 수 있습니다.

다음과 같은 조건을 따라야 합니다:



저작자표시. 귀하는 원 저작자를 표시하여야 합니다.



비영리. 귀하는 이 저작물을 영리 목적으로 이용할 수 없습니다.



변경금지. 귀하는 이 저작물을 개작, 변형 또는 가공할 수 없습니다.

- 귀하는, 이 저작물의 재이용이나 배포의 경우, 이 저작물에 적용된 이용허락조건을 명확하게 나타내어야 합니다.
- 저작권자로부터 별도의 허가를 받으면 이러한 조건들은 적용되지 않습니다.

저작권법에 따른 이용자의 권리와 책임은 위의 내용에 의하여 영향을 받지 않습니다.

이것은 [이용허락규약\(Legal Code\)](#)을 이해하기 쉽게 요약한 것입니다.

[Disclaimer](#)



Liraglutide Encapsulated Triple Layer Microneedle (TLM) for Treatment of Obesity

Seorin Juhng

The Graduate School

Yonsei University

Department of Biotechnology

Liraglutide Encapsulated Triple Layer Microneedle (TLM) for Treatment of Obesity

A Master's Thesis
Submitted to the Department of Biotechnology
and the Graduate School of Yonsei University
in partial fulfillment of the
requirements for the degree of
Master of Engineering

Seorin Juhng

February 2021

This Certifies that the Master's thesis of

Seorin Juhng is approved.

Thesis Supervisor: Hyungil Jung

Jae-Kwan Hwang: Thesis Committee Member

Hyuk Wan Ko: Thesis Committee Member

The Graduate School

Yonsei University

February 2021

감사의 글

다사다난했던 석사 학위 과정을 마치고 드디어 졸업하고 사회로 떠나게 되었습니다. 2년 동안 저 개인의 학문적 소양 뿐만 아니라 정신적으로도 많이 성숙하게 되었습니다.

먼저 저를 지지해주고 항상 아낌없는 사랑을 주셨던 부모님, 부모님 모시느라 고생했던 동생, 항상 내 옆에 있어준 사랑하는 남자 친구, 존재 자체로 감사한 테오에게 감사합니다.

정형일 교수님의 가르침 덕분에 제가 더 성숙하고 발전할 수 있었고, 연구자가 지녀야 할 열정과 태도를 항상 마음속에 깊이 새기고 살겠습니다. 또한, 학위논문 심사위원이셨던 황재관 교수님, 고혁완 교수님께도 감사합니다.

다같이 고생했던 연구실 사람들, 모두 감사합니다. 나와 같이 학위 과정을 함께 했던 동기 정윤이, 네가 있어서 항상 든든했고 배울 점도 많은 친구라 좋았다. 항상 힘든 일을 있을 때마다 도와주고 맛있는 것도 많이 사준 혜수, 뼈와 살이 되는 조언을 해 준 수용, 민규 오빠, 물건 찾거나 고치는 일에 항상 솔선수범해서 도와준 재홍 오빠, 쯔쯔 동기 준민이, 실험 막힐 때마다 알려주고 도와줬던 치송 유성 감사합니다. 하나를 가르치면 열을 아는 똑똑하고 대견한 지우, 찬솔, 지혜, 학부생이었던 수원, 정인, 덕영, 승현, 경진도 고생 많았다. 공동 연구하느라 함께 고생했던, 지은, 지현 쌤께도 감사드리고 싶습니다.

졸업 과정 중 나의 핵심수험급 잠수를 견디고 교우 관계를 유지해 준 천사 소영, 다영, 지영, 혜정 언니, 내 취업에 지대한 공을 준 은지, 모두 감사합니다.

초창기 주bic 인턴할 때 가르쳐주느라 고생한 건우, 현준, 수현에게도 감사합니다. 항상 천사같은 지영 선생님께도 감사해요.

TABLE OF CONTENTS

LIST OF FIGURES.....	III
ABSTRACT	IV
1. INTRODUCTION.....	1
2. MATERIALS AND METHODS	6
2.1. Fabrication of TLMs	6
2.2. Fracture force analysis	7
2.3. Skin penetration analysis on pig cadaver skin	7
2.4. <i>In vitro</i> distribution analysis of TLMs on agarose gel	9
2.5. <i>In vivo</i> liraglutide administration	9
2.6. Histology	10
2.7. Oil red O staining	11
3. RESULTS AND DISCUSSION	12
3.1. Fabrication and application of TLM	12
3.2. Optimization of the first layer	15
3.3. Volume optimization of the second layer	18
3.4. Optimization of the third layer.....	21

3.5.	Fracture force analysis	24
3.6.	<i>In vitro</i> skin penetration test.....	26
3.7.	<i>In vitro</i> distribution on agarose gel	28
3.8.	<i>In vivo</i> skin penetration test.....	31
3.9.	Efficacy of liraglutide loaded TLM patch in HFD induced obesity mouse model	33
3.10.	Amelioration of liver steatosis by liraglutide loaded TLM patch in HFD-induced obesity mice.....	36
4.	CONCLUSIONS	38
	REFERENCES	40
	ABSTRACT IN KOREAN	45

LIST OF FIGURES

	Page
Figure 1. Schematic illustration of fabrication and administration of TLM	14
Figure 2. Optimization of the first layer	17
Figure 3. Effect of the volume of the second layer	20
Figure 4. The third layer analysis	23
Figure 5. Fracture force measurement	25
Figure 6. <i>In vitro</i> skin penetration test of TLM	27
Figure 7. <i>In vitro</i> agarose gel diffusion test	27
Figure 8. <i>In vivo</i> skin penetration test	30
Figure 9. <i>In vivo</i> efficacy of Lira-TLM	32
Figure 10. Effect of Lira-TLM on hepatic steatosis	35

ABSTRACT

Liraglutide Encapsulated Triple Layer Microneedle (TLM) for Treatment of Obesity

Seorin Juhng

Department of Biotechnology

The Graduate School

Yonsei University

Obesity is a chronic metabolic disease prevalent worldwide, causing complications that affect quality of life and longevity. Liraglutide is the glucagon-like peptide-1 receptor agonist which suppresses appetite and increase insulin secretion. Here we suggest a novel core-encapsulated liraglutide dissolving microneedle (TLM) for painless and patient-friendly

long-term obesity treatment. In contrast to previous anti-obesity DMN approaches, TLM is consisted of triple layer: pedestal first layer, drug encapsulated core layer, shielding and protecting third layer. In order to increase the manufacturing efficiency and reproducibility, the process of each layer was analyzed, and the specification and manufacturing condition of TLM were optimized. Liraglutide encapsulated TLM was administered to C57BL mice twice a day for 2 weeks to observe the efficacy of obesity treatment. TLM with liraglutide reduced body weight and gonadal fat by 20% and 44%, respectively, compared to the control group.

It is the first attempt, to the best of our knowledge, to load an obesity treatment peptide medicine on a triple-layer microneedle for long-term administration. In the future, application and development of TLM for encapsulating various types of biologics to treat other disease should be conducted.

Keyword: Transdermal drug delivery, Dissolving microneedle, Liraglutide, Obesity, Core microneedle, GLP-1 receptor agonist, Biologics

1. INTRODUCTION

Obesity, defined as a body mass index (BMI) $\geq 30 \text{ kg/m}^2$, [1] has increased due to a sedentary lifestyle and lack of physical activity in modern society [2]. According to the World Health Organization, 39% of the world's adult population were overweight, and obesity has become a major concern for public healthcare programs over the past decades [3]. Obesity is considered as a significant risk factor for increased morbidity and mortality, predominantly from cardiovascular disease and diabetes [4], but also cancer [5] and chronic diseases, including osteoarthritis [6], gallbladder disease [7], sleep apnea [8], and depression [9]. Although improved lifestyle habits such as diet control and exercise therapy can help the treatment of obesity [10][11], active drug therapy is required when the effect of improving lifestyle is insufficient.

Representative anti-obesity drugs include noradrenergic activator (phentermine, diethylpropion, phendimetrazine, benzphetamine), gastrointestinal lipase inhibitor (orlistat), serotonin receptor activator (lorcaserin), and glucagon-like peptide-1 (GLP-1) receptor agonist (liraglutide) [12]. The comparing study showed that the effect of weight loss appeared in the order of phentermine/topiramate combination, liraglutide, naltrexone/bupropion, lorcaserin, and orlistat [13]. Most of the existing

obesity medications are classified as psychotropic drugs and have cardiovascular and neuropsychiatric side effects.

Liraglutide prevents cardiovascular disease and is safe from psychosis [14] because it is an appetite control substance to lose weight by increasing satiety and reducing hunger and food intake [15][16] in the human body [6][7]. Because of these advantages over the other drugs, liraglutide has been widely used to make significant weight loss [17] via subcutaneous (SC) injection. Although liraglutide is administered once daily for 2 months due to 13 h half-life [18], this SC injection caused infection, metal waste, and pain resulting in patient compliance reduction [19]. Furthermore, repeated injections at the same site may lead to extensive localized amyloid deposition [20]. Since liraglutide is a peptide with high molecular weight (3751 Da), oral and transdermal delivery is limited due to the low bioavailability [21]. To solve these problems, the development of a minimally invasive and effective liraglutide delivery system is required.

Dissolving microneedle (DMN) is a novel transdermal drug delivery system that creates microscopic channels in the epidermis and upper dermis, and the encapsulated drug reaches the target tissue by dissolution or degradation, ensuring virtually painless and highly efficient drug delivery.

Since it is in the form of an adhesive patch, even elderly and infirm patients can apply it by self-administration without healthcare providers' help [22]. By taking the advantages of DMN, various novel DMN delivery strategies for obesity treatment have been developed. Than et al. and Zhang et al. developed anti-obesity DMN to deliver adrenoceptor agonist, CL316243, and convert white fat to brown fat [23][24]. Dangol et al. introduced caffeine-loaded DMN to stimulate lipolysis leading to a weight loss of 12.8% in high fat diet-induced obese mice [23]. However, drugs encapsulated in these DMNs are mostly sympathetic agents, which are psychoactive. Considering the effect of liraglutide on weight loss, the encapsulation of liraglutide into DMN has been the goal for the minimally invasive treatment of obesity. However, liraglutide loaded DMN has not been studied yet, because liraglutide, a high molecular weight peptide, may undergo a high-temperature process to solidify the structure [25][26], which causes liraglutide denaturation and low bioavailability during the DMN fabrication process. Therefore, to encapsulate and deliver liraglutide in the formulation of DMN, a novel approach that maintains liraglutide's activity during DMN fabrication and satisfies the required dosage during DMN delivery is required for the treatment of obesity.

In this study, we propose a novel DMN system, namely ‘Liraglutide encapsulated triple layer system (TLM)’ which is composed of triple layers to improve the drug efficacy and bioavailability; the first base layer that serves as foundation and supporting of complete insertion, the second core layer designed to load drug, and the third shield layer which covers and protects the encapsulated drug. Unlike previous DMN systems, which drugs are exposed to outer environment, drug in TLM is shielded, therefore preventing from activity loss of encapsulated drug during fabrication and storage via denaturation or degradation. We analyzed and optimized the fabrication of TLM system; skin permeability according to the height of the base layer, the maximum active drug loading in the core layer, the effect on the shield layer for the prevention of activity loss. To visualize and examine the function of TLM, we performed fracture force and skin penetration test using both pig cadaver skin and agarose gel. Furthermore, in vivo efficacy was observed via high-fat diet (HFD) induced obese mice experiment. We compared the therapeutic effect of liraglutide on obese mice from SC injection group and liraglutide loaded TLM group. Results indicate that TLM had a similar effect to those of SC injection. After two weeks application of liraglutide- loaded TLM, it has been shown 20.7% decrease in body weight

and fat mass in diet-induced obese mice compared to the control group. We envision that compared with the current delivery systems, TLMs provide efficient delivery and can improve patient compliance, thereby offering an effective alternative for treating patients with obesity.

2. MATERIALS AND METHODS

2.1. Fabrication of TLMs

To prepare the first droplet solution, 65% (w/w) hyaluronic acid (HA) (30kDa, medical-grade; UsCarepharm, Suwon, Korea) was dissolved in 3 mL distilled water. The solution was homogenized at 1500 rpm for 15 minutes in a planetary centrifugal mixer (ARV-310; THINKY Corporation, Tokyo, Japan). The viscous mixture was dispensed through a 40 gauge nozzle (Precision-solid nozzle, Musashi, Japan) by the air pressure of 110 kPa. The air pressure was produced by a compressor (Major V100, Airfactory, Korea) and controlled by a dispenser (ML-5000, Musashi, Japan). The syringes containing the HA solutions were arranged in a 3 x 7 array on the automated X, Y, and Z stage (SHOT mini 100-s, Musashi, Tokyo, Japan). The droplets were dried for at least 20 minutes in 25°C, 40% relative humidity.

For the core layer preparation, 65% (w/w) HA powder and 4% (w/w) liraglutide were dissolved in 1 mL of distilled water with 0.47 mg disodium hydrogen phosphate dihydrate and 4.67 mg propylene glycol. The solution was agitated at 1500 rpm for 15 minutes in the mixer for homogenization and centrifuged at 1952 g for degassing (Combi R515, Hanil, Korea). The core droplet solution was dispensed on top of the base layer through a 20

gauge nozzle with an air pressure of 150 kPa. For the shield layer's preparation, the same formulation as the base layer was used, and the viscous mixture was dispensed on the core layer through a 40 gauge nozzle with an air pressure of 100 kPa. A 3 x 7 array of triple-layered droplets were fabricated into liraglutide encapsulated TLMs via centrifugal lithography [27]. Centrifuge condition: 1952 g, acceleration rate as 9 m/s², deacceleration rate as 5 m/s², and running time as 4 minutes.

2.2. Fracture force analysis

TLMs were imaged via LEICA M165 FC (LEICA, Wetzlar, Germany). The mechanical fracture force of a single TLM was measured by a force test machine (Z0.5TN, Zwick/Roell, Ulm, Germany). TLM was attached to the stainless-steel station, and the sensor probe was pressed against the DMN at a speed of 3.6 mm/min at 0.02 N via an axial force.

2.3. Skin penetration analysis on pig cadaver skin

Skin insertion test of TLMs was conducted on a pig cadaver skin (surface area: 2.5 cm², thickness: 1 mm; CRONEX, Seoul, Korea) melted in the water bath at 37°C for 30 minutes and dried at room temperature for 10 minutes. Rhodamine B (479 Da, Sigma Aldrich, USA) encapsulated TLMs penetrated through the porcine skin, and the patch was attached to the skin

for 30 minutes with medical tape (Transpore Surgical Tape, 3M, St. Paul, MN, USA). Excess rhodamine B was wiped out with Kimtech (Kimtech science wipers, Yuhan Kimberly, Seoul, Korea), and the porcine skin was rinsed with distilled water. Perforations were observed using a stereomicroscope (M165FC, Leica Camera AG, Wetzlar, Germany) and a digital microscope camera (DFC450C, Leica Camera AG, Wetzlar, Germany).

TLM's quantitative determination was performed using a microplate reader (Victor X3, Perkin Elmer, Waltham, MA, USA). Diffusion of 50 µl (0.1% w/w) rhodamine B was visualized over the epidermis layer of pig cadaver skin for 30 minutes. Images were taken using a stereomicroscope (M165FC, Leica Camera AG, Wetzlar, Germany). The skin was gently wiped with Kimtech (Kimtech science wipers, Yuhan Kimberly, Seoul, Korea) to remove excess rhodamine B before each analysis. A stock solution of TLM was serially diluted from 0%, 12.5%, 25%, 50% and 100% ($R^2 \geq 0.99$) to prepare the calibration curve.

2.4. *In vitro* distribution analysis of TLMs on agarose gel

An agarose gel with a viscosity of 20% was prepared by mixing distilled water with a 5% agarose (Sigma Aldrich, USA). The gel was then allowed to polymerize in microwave for 3 min. TLMs were inserted into the 5% agarose gel and recorded using a LEICA (M165FC, Leica Camera AG, Wetzlar, Germany).

2.5. *In vivo* liraglutide administration

All animal experiments were guided by following with the guidelines and regulations for experimentation ethics of Yonsei Laboratory Animal Research Center (YLARC) and performed according to procedures approved by Institutional Animal Care and Use Committee (IACUC) at Yonsei University. All mice were accommodated under controlled room temperature (22-24°C) with a 12-hour light/dark cycle. Male C57BL/6J mice were purchased from Raon bio (Yongin, Korea). After 1-week adaptation to animal facility, all mice were fed high fat diet (HFD) containing 60% fat ad libitum for 6 weeks. All mice were weighted every week and the blood glucose levels were measured using a glucometer (Osang healthcare, Korea) as indicated.

The obese mice which had more than 30 g body weight were randomly divided into 5 groups: (a) An untreated group (negative control, n=4); (b) a liraglutide injection group (IP injection, 0.2 mg/kg liraglutide solution, positive control, n=4); (c) a saline injection group (IP injection, saline, negative control, n=4); (d) a liraglutide loaded TLM group (Lira-TLM, 0.2 mg/kg liraglutide, n=4); (e) an empty microneedle group (n=4). Obese mice were treated with patch twice a day (at 10:30 AM and 5:30 PM) for 15 days during the experiment and weighed every day to assess the effect of TLM on body weight.

2.6. Histology

Pieces of livers and gonadal fat tissues were fixed with formalin neutral buffered solution for overnight and paraffin embedded. Embedded tissue paraffin blocks were cut (6 μm) and hematoxylin and eosin (H&E) stain was subsequently followed. Images were taken using a microscope system (Leica DM750, Switzerland) with a Leica digital camera (ICC50) and imaging software (LAS version 4.12.0).

2.7. Oil red O staining

Livers were cut to small pieces and fixed with 10% formalin for overnight and OCT compound embedded. Frozen sections (10 μm) were prepared by standard cryostat procedures. Before Oil red O staining, sections were post-fixed with 10% formalin for 10 minutes and then, briefly washed with running tap water for 10 minutes. The sections were washed with 60% 2-propanol and counterstained with nuclei with hematoxylin. A LAS version 4.12.0 (Switzerland) of Leica DM750 microscope was used to microscopic examination, and the images were taken using a Leica digital camera (ICC50) at 10 x (ocular lens), 40 x (object lens) magnification.

3. RESULTS AND DISCUSSION

3.1. Fabrication and application of TLM

Schematic design of fabrication and administration of TLM was shown in Figure 1. TLM was fabricated with the following steps, i) first layer (base layer) preparation, ii) core layer (core layer) formation with liraglutide on the base layer, iii) and third layer (shield layer), which overlapped the base and core layers (Figure 1A). We adopted 30 kDa low molecular weight HA as a backbone polymer with anti-atrophic and anti-aging activity [28][29][30][31]. FITC-dextran was used as a green fluorescent dye for the base and the shield layer to visualize the differences between each layer. After dispensing the viscous mixture without liraglutide on a flat surface, the droplet was dried to prepare the base layer. The core layer with liraglutide was fabricated on the base layer. We utilized rhodamine B as a model drug to visualize the core structure due to its red fluorescent characteristic. In step iii) after dispensing the droplet covering base and core layer, centrifugal lithography was performed to fabricate TLM [27].

During the intradermal administration, the base layer helped the complete insertion, resulting in quantitative drug delivery. TLM's shield layer had the role of piercing the skin's stratum corneum and protecting the

core layer where the liraglutide was encapsulated. The shield layer began to dissolve first, then the core layer dissolved where the liraglutide was encapsulated. During the core layer's dissolution, liraglutide flowed into the interstitial fluid, entering the heart through capillaries, and underwent systemic circulation (Figure 1B). Liraglutide promoted insulin secretion, reduced blood glucose while protecting the cardiovascular system, and acted on the brain to suppress appetite via binding to GLP-1 receptor (Figure 1C). The bright-field and fluorescent images of each TLM step were shown in Figure 1 D-H. The core layer was successfully deposited on the base layer (Figure 1D), and the shield layer covered the base and the core layer (Figure 1E). After centrifugation, the fabricated TLM (Figure 1F) showed the separated red core layer protected by shield layer on base layer. The section image of the TLM clearly showed that the separated core layer was located at the core of the TLM (Figure 1G, right). We fabricated 4 x 7 arrays of TLM on a patch (Figure 1H). These data indicated that TLM could be fabricated in a stepwise manner via dispensing of each layer without mixing.

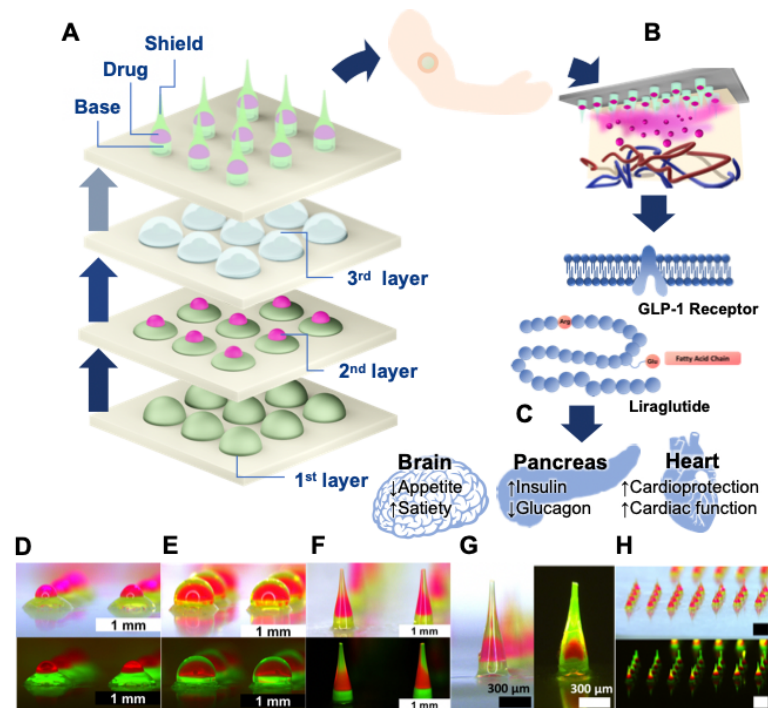


Figure 1. Schematic illustration of fabrication and administration of triple layer microneedle (TLM). (A) Fabrication process and treatment of obesity via transdermal liraglutide loaded TLM delivery. The second layer, which is combination of Hyaluronic Acid (HA) and liraglutide, is placed onto the first layer, and then shielded by the third layer. Needle shape patch is fabricated through centrifugal lithography. (B) Patch application and insertion into skin allowing diffusion of liraglutide after dissolution. (C) Effect of drug to multiple human organs. Liraglutide suppresses appetite by increasing satiety, increases insulin secretion while suppresses glucagon secretion. In heart, it increases cardioprotection and cardiac function. Bright-field (upper) and fluorescent (lower) images of (D) the second layer, (E) the third layer and (F) fabricated TLM. (G) Bright-field (left) and cross sectional (right) image of TLM. (H) Bright-field (upper) and fluorescent (lower) image of an array of TLM.

3.2. Optimization of the first layer

In the traditional DMN patch system, the complete insertion to the base of the DMN is difficult due to the skin elasticity and resistance of insertion at the base portion of DMN resulted in the inconsistent drug delivery [25]. Therefore, a variety of novel DMN approaches, such as two-layered DMNs [32][33][34][35] and arrowhead DMNs [36][37], which encapsulate the drug into the tip or the top part of the DMN, have been introduced for the quantitative delivery of encapsulated drug. Because the TLM was fabricated from the dispensed polymer by stepwise manner, the height optimization of the base layer was required for the quantitative drug delivery in TLM.

Because the base layer was fabricated after drying from the dispensed viscous HA solution, its height was controlled by the polymer concentration. As shown in Figure 2, the height of base layer decreased as the drying time increased due to the evaporation of solvent and thus shrinkage of the polymer during drying. After complete drying, the height of base layer increased from 150 μm to 275 μm as the concentration of HA increased from 65% to 75% [38]. This implied that the base layer can be easily controlled by changing the HA concentration. Although the base layer was essential for the quantitative delivery because of the incomplete insertion, minimum height

was required to maximize the drug loading in a limited volume of fixed length of DMN. Because the 65% of HA showed 150 μm height, which was widely used height for quantitative drug delivery in two-layer DMN^[39], HA 65% was set as the optimal concentration of the first layer for further TLM fabrication.

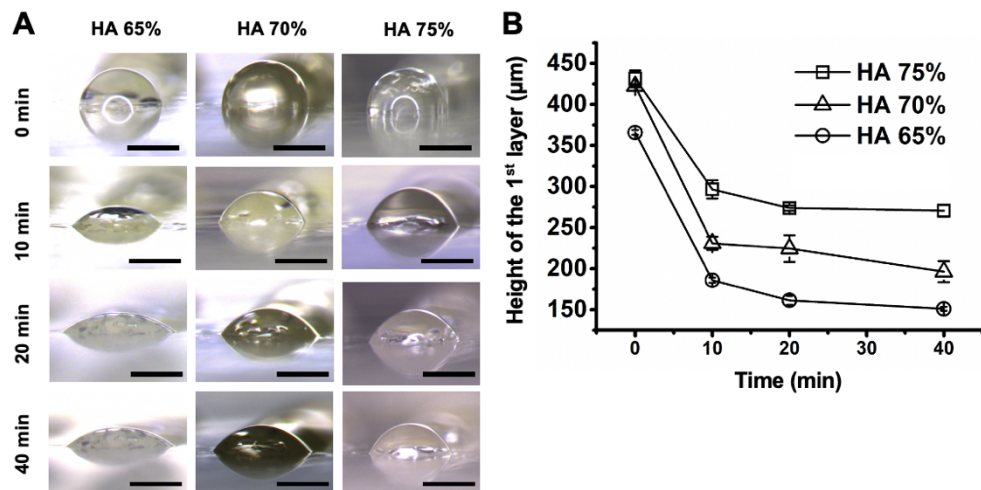


Figure 2. (A) Optical images of evaporation process of the first layer droplets by different time and hyaluronic acid (HA) concentration. Scale bars are 500 μm . (B) Plot of height of the first layer with different polymer concentration of HA 65%, 70% and 75%. Data are the mean \pm s.e.m (n=3).

3.3. Volume optimization of the second layer

In TLM, it is important to know the maximum amount of drug that can be loaded on the core layer for successful quantitative drug delivery. To optimize the core layer, the possibility of TLM fabrication and drug retention rate were measured according to the volume of the core layer with the concentration fixed (0.1% rhodamine B as a model drug and 65% HA) and the volume of the third droplet (130 nL) were fixed. As shown in side view and cross-section after core and shield layer fabrication (Figure 1A ii and iii), the more core layer was fabricated as the volume of the second droplet increased. Because TLM was fabricated via centrifugal lithography, in which the droplets were shaped into DMN by centrifugal force, the excess volume from droplets might fly off during fabrication [27]. This implied that if the core volume exceeded the third layer's shielding capacity, the third layer could not completely cover the core, resulting in the loss of the encapsulated drug. Therefore, optimization of the second droplet's volume was essential for accurate quantitative drug delivery with TLM.

As shown in TLM's cross-section image (Figure 3A iv), the core layer was not covered by the shield layer entirely when the TLM was fabricated from 25.6 and 33.6 nL second droplets. It was evident in TLM's cross-section

image, which was fabricated using a 33.6 nL second droplet. As shown in the image, most of the TLM volume showed red fluorescent at the TLM center. It implied that most of the third droplet (green) had flown off during centrifugal lithography and insisted that some of the second droplets might fly off. It was further confirmed by analyzing the drug amount in the core layer after TLM fabrication (Figure 3B). As the second droplet volume increased over 13.5 nL, the amount of drug in the core layer did not retain 100%, implying loss of some volume of the second layer during fabrication by centrifugal lithography. Because the second droplet leakage implied the failure of the third layer's shielding, implying the exposure of the core layer outside environment. Because TLM was designed to shield the core layer without drug loss during TLM fabrication, the second droplet's optimum volume to maximize the drug capacity without exposure to the outside was set as 13.5 nL (Figure 3B). For further studies, it is necessary to analyze the loading capacity according to the concentration, molecular weight and hydrophilicity of drug.

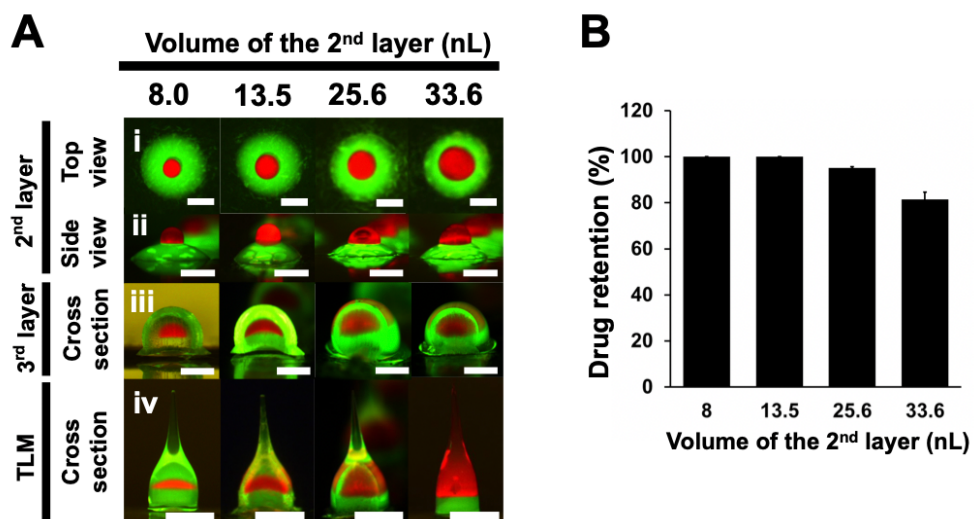


Figure 3. Effect of the volume of the second layer. (A) Fluorescent images of (i) top view of the second layer, (ii) side view of the second layer, sectioning images of (iii) the third layer and (iv) TLM by volume of the second layer. Scale bar is 300 μ m. (B) Preserved drug amount by increasing volume of the second layer. Data are the mean \pm s.e.m (n=3).

3.4. Optimization of the third layer

Body thickness of TLM differed depending on the third layer's volume, and it affected skin penetration (Fig. 4). After setting the volume of the second droplet as 13.5 nL, volume of the third droplet, which has a responsibility to pierce the stratum corneum of the skin and shield the core layer where the drug was encapsulated. When the third droplet volume was below 70 nL, it was not enough to prevent the core layer from being exposed to the outside, as shown in the cross-section image (Figure 4A). Because the third droplet volume of 100 and 130 nL were enough to cover the second droplet, shape comparison and skin penetration experiments were conducted with those groups. As explained earlier, in centrifugal lithography for the fabrication of TLM, the viscous form of the third droplet acts as a medium to shape into DMN by centrifugal force. When TLM was fabricated from 100 nL and 130 nL of the third droplet, TLM was successfully fabricated, showing the core layer at the center (Figure 4B and C) with different shapes at a fixed height (900 μ m). Shape comparison and skin penetration experiments were conducted with TLMs made with the third droplets of 100 and 130 nL volume. Because the TLM shape was controlled by the third droplet volume in centrifugal lithography, the TLM with a thicker shape was

produced from the third droplet with a volume of 130 nL. As a result, they had a thickness of 300 and 400 μm respectively (Fig. 4B,C). TLM with a 300 μm diameter had 100% efficiency of drug delivery than 95% for 400 μm (Figure 4D). As a result of considering these factors, a TLM with a volume of 13.5 nL and 100 nL for the second and the third droplet was selected as the final composition for further study.

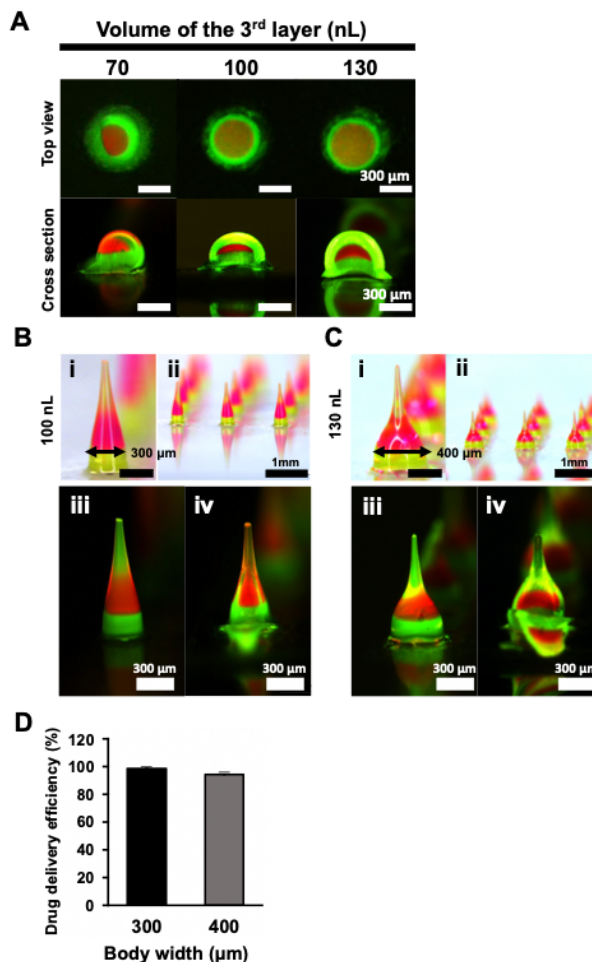


Figure 4. (A) Fluorescent images of the third layer with different volume. (B) Image of i) a single, ii) an array of TLM made with the 100 nL third layer. iii) Fluorescent image of i). iv) Cross sectional image of i). (C) Image of i) a single and ii) an array of TLM made with the 130 nL third layer. iii) Fluorescent image of i). iv) Cross sectional image of i). (D) Drug delivery efficiency of TLM. After the insertion, by measuring the degree of fluorescence in the patch, the amount of the drug transmitted through the skin was estimated. Data in (D) are the mean \pm s.e.m (n=3). Scale bars in (B)-(i) and (C)-(i) are 300 μm .

3.5. Fracture force analysis

Based on the optimal volume of 13.5 nL and 100 nL for the second and the third droplet, the liraglutide loaded TLM was fabricated with a length of $900 \pm 50 \mu\text{m}$ and a tip diameter of $30 \pm 5 \mu\text{m}$. The mechanical strengths of TLM loaded with model drug and liraglutide were compared. Rhodamine B, which had a red fluorescent, was selected as a model drug because it facilitated visibility in further experiments. Both TLM showed fracture as 0.28 N at a distance of 0.09 and 0.13 mm, indicating that the drug encapsulation did not affect TLM's strength (Figure 5) and TLM had enough strength to pierce the skin, both model drug-loaded and liraglutide encapsulated [40].

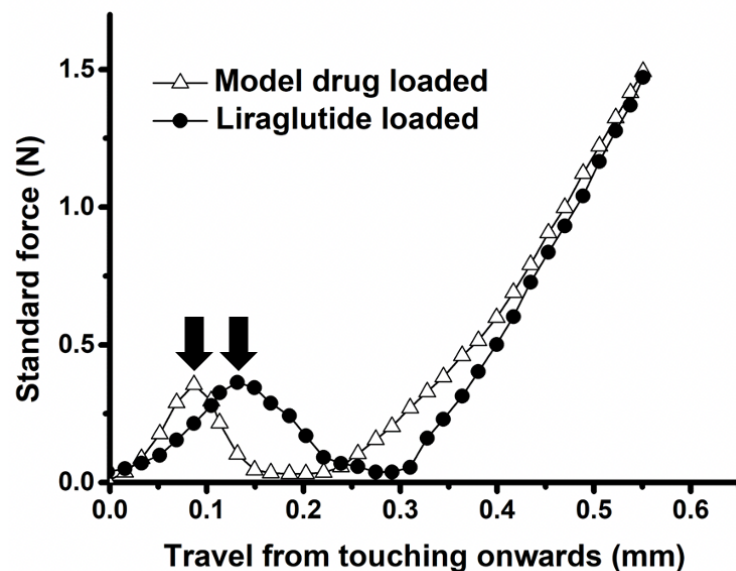


Figure 5. Fracture force measurement. Mechanical strength of a single Rhodamine B (model drug) and liraglutide loaded triple layer microneedle (TLM). Standard force was recorded by moving probe along the axial direction; the peaks of the graphs (black arrows) indicated the fracture force.

3.6. *In vitro* skin penetration test

In order to evaluate whether TLM is accurately inserted into the skin and to observe the diffusion pattern of the core layer in the subcutaneous layer, *in vitro* skin penetration test using pig cadaver skin was conducted (Fig. 6). Through centrifugal lithography, rhodamine B (red) encapsulated TLM was fabricated into 4 x 4 array with 0.1% rhodamine B and 65 % HA. After 10 min, dots of the 4 x 4 TLM array were observed on the pig cadaver skin (Figure 7A) indicating that the TLM arrays penetrated skins. To ensure the core layer's insertion into the epidermis, we analyzed the cross-section images using a fluorescence microscope (Figure 7B). Isolated red dots were observed below the skin surface, indicating the core layer's complete insertion. In the case of the core layer's incomplete insertion, the red dots might exist from the insertion site without isolation from the surface. This also implied that base layer promoted complete insertion, and the rhodamine B encapsulated in the core layer was safely transferred to the subcutaneous. As a result, *in vitro* skin penetration tests proved that the TLM could achieve complete insertion and efficient delivery of the core layer through the skin.

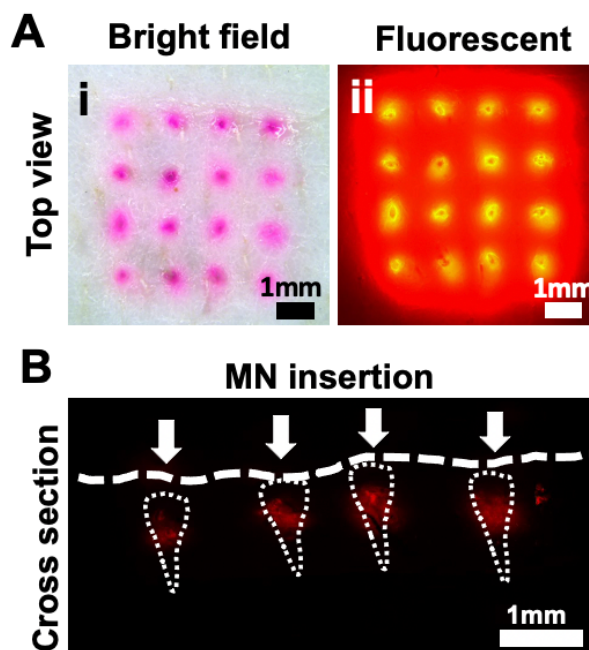


Figure 6. Skin penetration test of triple layer microneedle (TLM). (A) Top view of porcine skin after insertion of rhodamine B (red) loaded TLM observed under (i) bright field, (ii) fluorescent condition. (B) Cross-section image of porcine skin after insertion of rhodamine B loaded TLM showing the rhodamine B delivered subcutaneously.

3.7. *In vitro* distribution on agarose gel

To visually analyze the process of TLM dissolving under the skin, a single TLM encapsulated with a green fluorescent dye (FITC-dextran) on the base and shield layers and red fluorescent dye (rhodamine B) for the core layer (Core-Rho) was inserted into a transparent agarose gel (Figure 7). A single dissolving microneedle loaded with rhodamine B (Full-Rho) was utilized as a control group to compare and clarify the supporting effect of the first layer for complete insertion. The agarose gel was utilized as a substitute of human skin due to its similar viscoelastic properties and moisture content with human skin [41]. As shown bright field and fluorescent images of 1 seconds, the core layer was clearly separated from the base layer and shield layer and covered by shield layer. After 1 to 2 seconds of insertion, diffusion of green fluorescence was observed showing the shield layer dissolution. Also, the isolated red in bright field and isolated red fluorescence in agarose was observed indicating the complete insertion of the core layer. In addition to this, the green base layer at the site of insertion in fluorescent image clearly indicated this complete insertion of core layer of TLM into agarose. In Full-Rho group, the drug is exposed to the agarose surface, suggesting a possibility of incomplete insertion. Therefore the first layer of TLM could facilitate the complete insertion of loaded drug, serving as a backing layer.

This data matched the result of the complete insertion of the TLM in *in vitro* insertion analysis using pig cadaver skin (Figure 6B.). In Core-Rho group, after 5 to 10 seconds, red fluorescence started to smear as a result of dissolving of the core layer carrying rhodamine B. Green fluorescent dye diffused into the gel while time passed by and indicated that the remaining shield layer was almost invisible. The fluorescence of the core layer was also weakened at 30 seconds, indicating that the encapsulated drug had diffused into the gel. Although agarose gel had a similar viscoelastic property and moisture content with human skin, the dissolving rate would vary according to *in vivo* conditions, such as temperature, moisture content, age and skin conditions of individuals. Therefore, further research is required to analyze the dissolution time of target drugs delivered via TLMs.

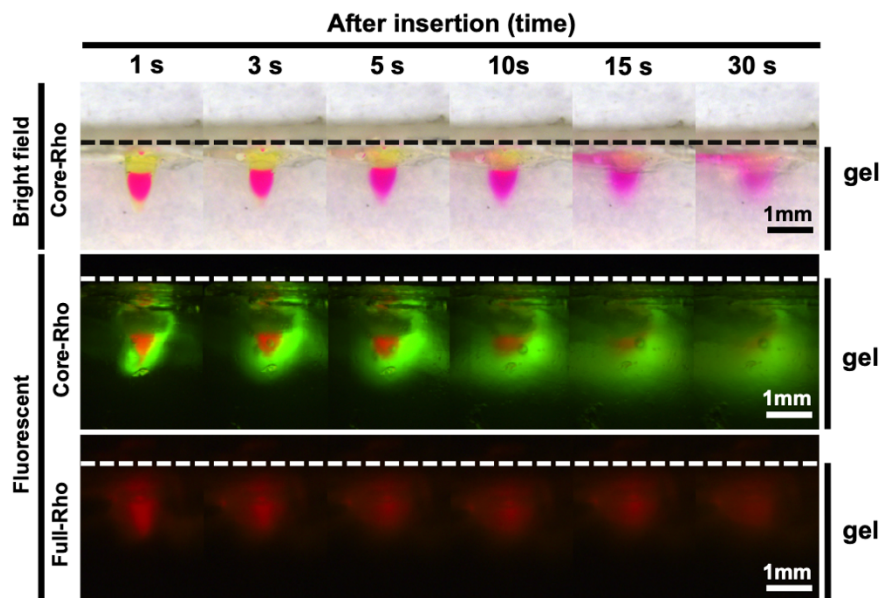


Figure 7. Bright field and fluorescent images of rhodamine B (red) loaded triple layer microneedle (TLM) insertion in an agarose gel. (green fluorescent; FITC-dextran. Core-Rho; rhodamine B was loaded in the core layer only. Full-Rho; rhodamine B was dissolved throughout the microneedle.) After 1 seconds of insertion, the FITC-dextran component constituting base and shield layer began to dissolve and emitted green fluorescence. At 3 to 5 seconds, the core layer carrying rhodamine B also started to dissolve.

3.8. *In vivo* skin penetration test

For the *in vivo* skin penetration test, TLM patches were applied in the back of C57BL mice twice a day for 2 weeks. After applying the patch, the C57BL mice were wrapped with bandage tape and allowed to act freely for 10 min (Figure 8A). After 10 min, the insertion marks and wounds on the skin surface of the mice were examined. There were no visible wounds such as redness and swelling, and when observed with bright-field and fluorescence microscopes, it was found that all of the TLMs were transmitted into the skin (Figure 8B, C). These implied that TLM could be applied for long-term *in vivo* liraglutide administration for treatment of obesity without any skin irritation.

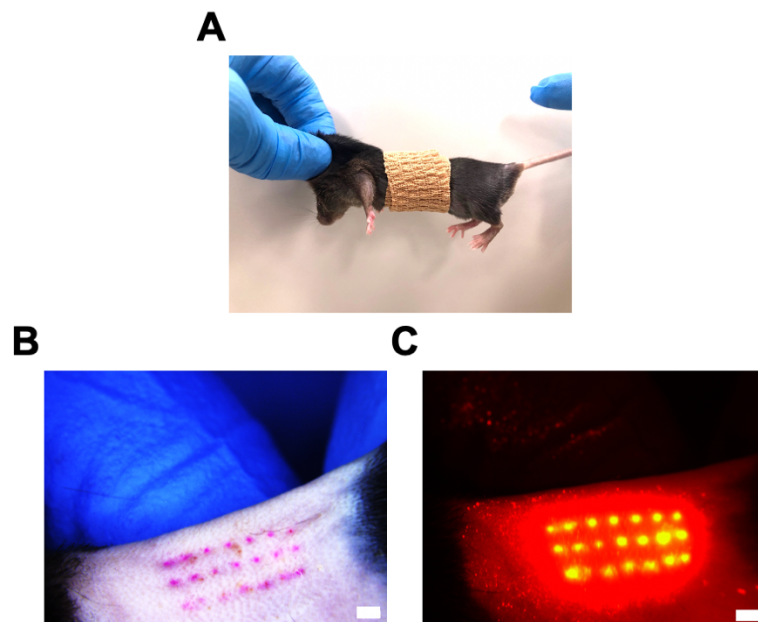


Figure 8. *In vivo* skin penetration test. (A) A C57BL mouse wrapped in bandage tape. (B) Mouse skin surface after applying rhodamine B (pink) encapsulated TLM patch for 10 minutes. (D) Fluorescent image of mouse skin surface after 10 minutes of TLM patch administration. Scale bars are 1 mm.

3.9. Efficacy of liraglutide loaded TLM patch in HFD induced obesity mouse model

To examine the *in vivo* efficacy of liraglutide-loaded TLMs in body weight control, we used HFD induced obesity mouse model. Briefly, 7 weeks old C57BL/6J mice were fed HFD for 6 weeks to make them obese and treated liraglutide with TLM patches or injection twice a day (Figure 9A). Body weights were measured a daily base for 2 weeks and compared with normal saline (Saline-IP) or liraglutide injection (Lira-IP) group and empty TLM patch (Blank-TLM) applied group as a control for TLMs (Lira-TLM). In 2 weeks application to obese mice, body weight percentage of Lira-IP group and Lira-TLM group were significantly reduced compared to the control group (Figure 9B). Significant reduction of body weight was observed at day 5 in the Lira-IP group and in the Lira-TLM group. Both of them showed similar efficacy as much as 20% decrease in body weight as shown Figure 9B. The fat tissue in the mice were analyzed in Figure 9C. Gross appearance of gonadal fat pad showed significantly reduced in fat mass in Lira-TLM and Lira-IP. HFD-induced obese mice receiving liraglutide-injection lose 45% and liraglutide-loaded TLMs lost 44% of gonadal fat (GF) pad weight compared to non-treated HFD-induced obesity

mice (Figure 9E). To further examine the effect of lowering fat mass in gonadal fat pad by Lira-TLM, we analyzed the histological changes in gonadal white adipose tissue. We quantified the number and size of gonadal adipocytes. GF cell number increased in Lira-IP and Lira-TLM group (Figure 9D) relative to controls but the diameter of GF cells decreased in liraglutide-treated groups (Figure 9F). These results showed that the new liraglutide encapsulated TLM effectively controled the body weight and composition in HFD induced obesity mouse model.

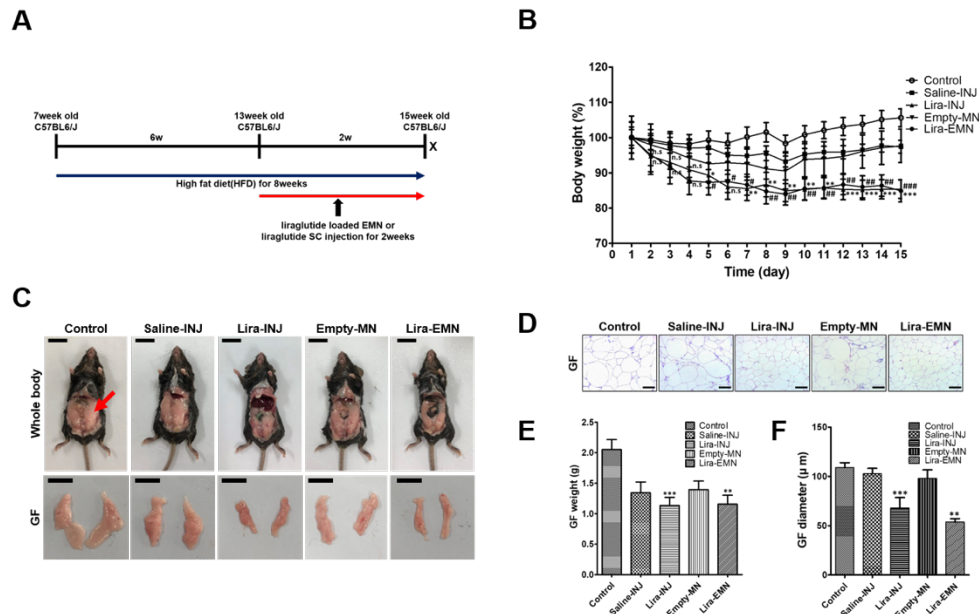


Figure 9. Efficacy of liraglutide loaded TLM patch in HFD induced obesity mouse model. (A) Schematic diagram of experiments using HFD induced obesity mouse model. (B) Body weights in each group ($n=4-7$) were monitored for 15 days. (C) Representative image of gross anatomy and gonadal fat (GF) pad of liraglutide treated or control mice (scale bars: 2cm). Red arrow indicates the accumulated gonadal fat tissue. (D) Representative image of histological analysis of gonadal white adipose tissue. Scale bar: 100 μ m. (E) WAT(GF) weights WAT(GF) ($n=4-7$). (F) Measurement of gonadal white adipose tissue ($n=3$). Data are presented as mean \pm SEM, *, $P < 0.05$, **, $P < 0.01$, ***, $P < 0.001$ for Lira-IP group, #, $P < 0.05$, ##, $P < 0.01$, ###, $P < 0.001$ for Lira-TLM group. All groups were compared with the control group. GF: gonadal fat

3.10. Amelioration of liver steatosis by liraglutide loaded TLM patch in HFD-induced obesity mice.

Since obesity and fatty liver disease is one of the most common associated diseases, it has been well-known that obese mice also develop hepatic steatosis. To determine the effect of Lira-TLM on the hepatic steatosis, histological analysis of liver were performed (Figure 10). The result showed that control obese mice had lipid droplet vacuoles in their livers, suggesting hepatic steatosis. These hepatic steatosis were improved by liraglutide treatment in Lira-TLM and Lira-IP. The liver weigh of Lira-IP group decreased 35.4% compared to saline-injection group, and Lira-TLM group decreased 20.2% compared to empty-MN group. These results indicated that Lira-TLM group had similar efficacy in improving the hepatic steatosis to Lira-IP. We further examined the extent of lipid droplet formation in liver by Oil red O staining (Figure 10A). However, the Oil red O positive vacuoles were detected in control groups, these vacuoles were reduced or not observed in liraglutide applied groups. These results suggested that the Lira-TLM could improve metabolism in obese mouse model system.

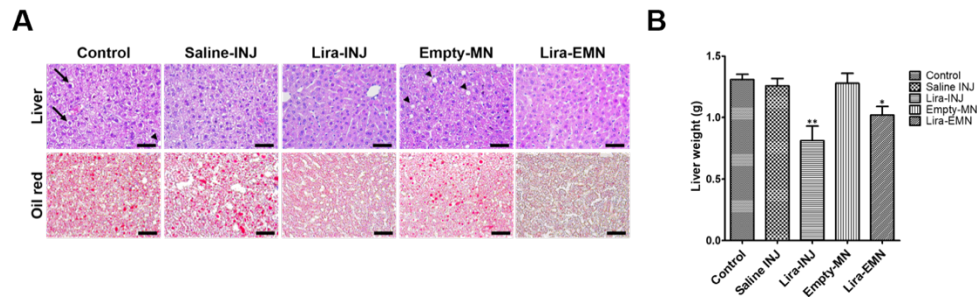


Figure 10. Liraglutide encapsulated TLM patch protects mice from HFD-induced hepatic steatosis. (A) Representative H&E staining of liver in each group. H&E staining shows lipid droplets accumulation (top panel). Arrows denote for massive macrosteatosis and arrowheads for microsteatosis. Lipid droplets accumulation confirmed by Oil Red O (ORO) staining (bottom panel). Scale bars: 50 μ m (B) Liver weight in each group (n=4). Data are presented as mean \pm SEM, *, P < 0.05, **, P < 0.01, ***, P < 0.001 for Lira-IP group, #, P < 0.05, ##, P < 0.01, ###, P < 0.001 for Lira-TLM group. All groups were compared with the control group.

4. CONCLUSIONS

This study proposed a novel liraglutide encapsulated triple layer microneedle (TLM) for the long-term treatment of obesity that is less painful and patient-friendly. Contrary to the traditional anti-obesity microneedle approach, TLM is composed of the first layer that acts as a support and aids in complete skin insertion, the core layer that loads the drug, and the third layer that shields and protects the core layer. In order to analyze and optimize the manufacturing process of the TLM system, the height of the first layer and skin permeability according to the polymer concentration, the maximum drug loading volume of the core layer, and the final TLM body thickness according to the volume of the third layer were studied.

Based on these results, the optimized specifications and manufacturing conditions of TLM were established for effective and quantitative drug delivery. For TLM to successfully penetrate the skin, the first layer should be a hyaluronic acid polymer with a concentration of 65% (w/w), the height should be 150 μm , and the volume of the core layer should be 13.5 nL. Besides, when the volume of the third layer was less than 100 nL, the body width of TLM became 300 μm , and it showed 100% skin penetration. Liraglutide encapsulated TLM was administered to C57BL mice twice a day

for 2 weeks to observe efficacy of obesity treatment. Lira-TLM reduced the body weight and gonadal fat by 20% and 44% each compared to the control group of C57BL/6J mice.

In conclusion, we presented the optimization of the TLM fabrication condition for development of an effective drug delivery system. Our study has proved that TLM could promote a modified human hormone release system for long-term daily administration, with relatively high patient compliance than injection. Research also showed the potential to utilize the TLM to effectively load different kinds of biomacromolecules to cure other diseases.

REFERENCES

- [1] *Physical Status: The Use and Interpretation of Anthropometry. Report of a WHO Expert Committee*, Switzerland, **1995**.
- [2] M. Á. Martínez-González, J. Alfredo Martínez, F. B. Hu, M. J. Gibney, J. Kearney, *Int. J. Obes.* **1999**, *23*, 1192.
- [3] M. T. Bassett, S. Perl, *Am. J. Public Health* **2004**, *94*, 1477.
- [4] S. E. Kahn, R. L. Hull, K. M. Utzschneider, *Nature* **2006**, *444*, 840.
- [5] G. A. Colditz, L. L. Peterson, *Clin. Chem.* **2018**, *64*, 154.
- [6] D. J. Hunter, S. Bierma-Zeinstra, *Lancet (London, England)* **2019**, *393*, 1745.
- [7] X. Pi-Sunyer, *Postgrad. Med.* **2009**, *121*, 21.
- [8] A. Romero-Corral, S. M. Caples, F. Lopez-Jimenez, V. K. Somers, *Chest* **2010**, *137*, 711.
- [9] Y. Milaneschi, W. K. Simmons, E. F. C. van Rossum, B. W. Penninx, *Mol. Psychiatry* **2019**, *24*, 18.
- [10] A. Rodríguez-Martín, J. P. Novalbos Ruiz, J. M. Martínez Nieto, L.

- Escobar Jiménez, *Nutr. Hosp.* **2009**, *24*, 144.
- [11] E. M. Matheson, D. E. King, C. J. Everett, *J. Am. Board Fam. Med.* **2012**, *25*, 9.
- [12] H. L. Daneschvar, M. D. Aronson, G. W. Smetana, *Am. J. Med.* **2016**, *129*, 879.e1.
- [13] D. M. Williams, A. Nawaz, M. Evans, *Diabetes Ther.* **2020**, *11*, 1199.
- [14] R. Howell, A. M. Wright, J. N. Clements, *Diabetes. Metab. Syndr. Obes.* **2019**, *12*, 505.
- [15] N. Mikhail, *Curr. Hypertens. Rev.* **2019**, *15*, 64.
- [16] B. Rolin, M. O. Larsen, C. F. Gotfredsen, C. F. Deacon, R. D. Carr, M. Wilken, L. B. Knudsen, *Am. J. Physiol. Endocrinol. Metab.* **2002**, *283*, E745.
- [17] L. V. Jacobsen, A. Flint, A. K. Olsen, S. H. Ingwersen, *Clin. Pharmacokinet.* **2016**, *55*, 657.
- [18] S. H. Jackson, T. S. Martin, J. D. Jones, D. Seal, F. Emanuel, *P T* **2010**, *35*, 498.
- [19] L. Cea-Calvo, L. Carmona, J. Calvo-Alén, *Adv. Ther.* **2017**, *34*, 2173.

- [20] C. O. Martins, C. Lezcano, S. S. Yi, H. J. Landau, J. R. Chapman, A. Dogan, *Haematologica* **2018**, *103*, e610.
- [21] J. Shaji, V. Patole, *Indian J. Pharm. Sci.* **2008**, *70*, 269.
- [22] J. J. Norman, J. M. Arya, M. A. McClain, P. M. Frew, M. I. Meltzer, M. R. Prausnitz, *Vaccine* **2014**, *32*, 1856.
- [23] M. Dangol, S. Kim, C. G. Li, S. Fakhraei Lahiji, M. Jang, Y. Ma, I. Huh, H. Jung, *J. Control. Release* **2017**, *265*, 41.
- [24] L. Y. Chu, S.-O. Choi, M. R. Prausnitz, *J. Pharm. Sci.* **2010**, *99*, 4228.
- [25] S. F. Lahiji, M. Dangol, H. Jung, *Sci. Rep.* **2015**, *5*, 1.
- [26] M.-C. Chen, Z.-W. Lin, M.-H. Ling, *ACS Nano* **2016**, *10*, 93.
- [27] H. Yang, S. Kim, G. Kang, S. F. Lahiji, M. Jang, Y. M. Kim, J. M. Kim, S. N. Cho, H. Jung, *Adv. Healthc. Mater.* **2017**, *6*, 1.
- [28] M. Litwiniuk, A. Krejner, M. S. Speyrer, A. R. Gauto, T. Grzela, *Wounds – a Compend. Clin. Res. Pract.* **2016**, *28*, 78.
- [29] G. Huang, H. Huang, *Drug Deliv.* **2018**, *25*, 766.
- [30] R. C. Gupta, R. Lall, A. Srivastava, A. Sinha, *Front. Vet. Sci.* **2019**, *6*,

192.

- [31] R. Campiche, E. Jackson, G. Laurent, M. Roche, S. Gougeon, P. Séroul, S. Ströbel, M. Massironi, M. Gempeler, *Int. J. Pept. Res. Ther.* **2020**, *26*, 181.
- [32] Y. Hao, Y. Chen, M. Lei, T. Zhang, Y. Cao, J. Peng, L. Chen, Z. Qian, *Adv. Ther.* **2018**, *1*, 1800008.
- [33] A. P. Raphael, T. W. Prow, M. L. Crichton, X. Chen, G. J. P. Fernando, M. A. F. Kendall, *Small* **2010**, *6*, 1785.
- [34] K. Fukushima, A. Ise, H. Morita, R. Hasegawa, Y. Ito, N. Sugioka, K. Takada, *Pharm. Res.* **2011**, *28*, 7.
- [35] M.-C. Chen, M.-H. Ling, S. J. Kusuma, *Acta Biomater.* **2015**, *24*, 106.
- [36] D. D. Zhu, Q. L. Wang, X. B. Liu, X. D. Guo, *Acta Biomater.* **2016**, *41*, 312.
- [37] M.-C. Chen, S.-F. Huang, K.-Y. Lai, M.-H. Ling, *Biomaterials* **2013**, *34*, 3077.
- [38] J. Um, Development of Disposable Dissolving Microneedle Applicator for Efficient Transdermal Delivery, 연세대학교,

일반대학원, 2020.

- [39] Q. L. Wang, X. P. Zhang, B. Z. Chen, X. D. Guo, *Mater. Sci. Eng. C* **2018**, 83, 143.
- [40] S. P. Davis, B. J. Landis, Z. H. Adams, M. G. Allen, M. R. Prausnitz, *J. Biomech.* **2004**, 37, 1155.
- [41] A. K. Dąbrowska, G.-M. Rotaru, S. Derler, F. Spano, M. Camenzind, S. Annaheim, R. Stämpfli, M. Schmid, R. M. Rossi, *Ski. Res. Technol. Off. J. Int. Soc. Bioeng. Ski. [and] Int. Soc. Digit. Imaging Ski. [and] Int. Soc. Ski. Imaging* **2016**, 22, 3.

ABSTRACT IN KOREAN

비만 치료를 위한 리라글루티드 탑재 삼중층 마이크로니들

비만은 전세계적으로 만연한 만성 대사 질환으로 삶의 질과 수명에 영향을 미치는 합병증의 원인이 된다. 리라글루티드 (Liraglutide)는 식욕을 억제하고 인슐린 분비를 증가시키는 글루카곤 유사 펩티드-1 수용체 작용제이다. 일반적으로 비만치료제는 장기 투여가 필요하지만 리라글루티드의 경우 단백질 약물로서 경구 투여 시 생체이용률이 감소하므로 피하주사로 투여한다. 이 과정에서 감염 및 통증으로 인해 환자 편의성이 감소한다. 본 연구에서는 최소침습적이고 환자친화적인 비만 장기 치료를 위한 새로운 리라글루티드 탑재 삼중층 마이크로니들 (TLM)을 제안한다. 이전의 항 비만 마이크로니들 접근법과 달리 TLM은 지지대 역할을 하며 완전한 피부 삽입을 돋는 1층, 약물을 탑재하는 2층, 2층을 차폐 및 보호하는 3층으로 구성된다. 제작 성공률과 재현율 증대를 위해 각 층 별 공정 과정을 분석하고 약물 전달에 최적화된 TLM의 규격 및 제작 조건을 수립하였다. TLM이 피부에 성공적으로 침

투하려면 1층이 농도 65% (w/v)의 히아루론산 고분자 소재로 높이가 $150 \mu\text{m}$ 이상이어야 하며, 2층의 부피가 13.5 nL 이하여야 한다. 또한 3층의 부피가 100 nL 이하일 때 TLM의 몸체 두께는 $300 \mu\text{m}$ 가 되며, 100% 피부 투과율을 보인다. 리라글루티드 탑재 TLM을 C57BL 마우스에 2 주 동안 하루에 두 번 투여하여 비만치료의 효능을 관찰하였다. 리라글루티드 탑재 TLM은 대조군에 비해 체중과 생식선 지방을 각각 20 % 및 44 % 감소시켰다.

결론적으로 우리는 효과적인 약물 전달 시스템 개발을 위한 TLM 제작 조건의 최적화를 제시하였다. 또한, 2 주 간의 장기 일일 적용 실험을 통해 웹타이드를 탑재한 TLM이 주사를 대체하여 보다 높은 환자 친화성을 갖는 약물 전달 시스템 개발의 가능성을 입증하였다. 장기 투여용 웹타이드 비만치료제를 삼중층 마이크로 니들에 탑재한 것은 본 연구에서 최초로 시도하는 것으로, 향후 TLM을 다양한 종류의 생체 고분자를 효과적으로 탑재하여 다른 질병을 치료하는 연구가 진행되어야 할 것이다.